

1 *Supplemental Information for*

2 **Revisiting the high tropospheric ozone over Southern Africa:**  
3 **overestimated biomass burning and underestimated anthropogenic**  
4 **emissions**

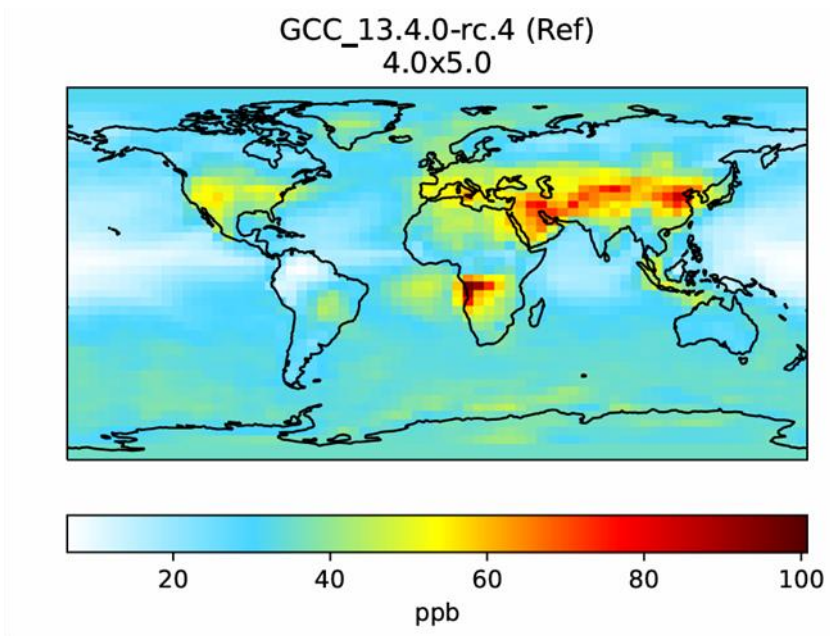
5 Yufen Wang<sup>1</sup>, Ke Li<sup>1\*</sup>, Xi Chen<sup>1</sup>, Zhenjiang Yang<sup>1</sup>, Minglong Tang<sup>1</sup>, Pascoal M.D. Campos<sup>2</sup>, Yang  
6 Yang<sup>1</sup>, Xu Yue<sup>1</sup>, and Hong Liao<sup>1</sup>

7 <sup>1</sup>Jiangsu Key Laboratory of Atmospheric Environment Monitoring and Pollution Control, Jiangsu Collaborative  
8 Innovation Centre of Atmospheric Environment and Equipment Technology, Joint International Research Laboratory of  
9 Climate and Environment Change, School of Environmental Science and Engineering, Nanjing University of Information  
10 Science and Technology, Nanjing, China

11 <sup>2</sup>CNIC-Centro Nacional de Investigação Científica, Ministério Do Ensino Superior Ciência, Tecnologia e Inovação,  
12 Avenida Ho Chi Minh N° 201, Luanda, Angola

13

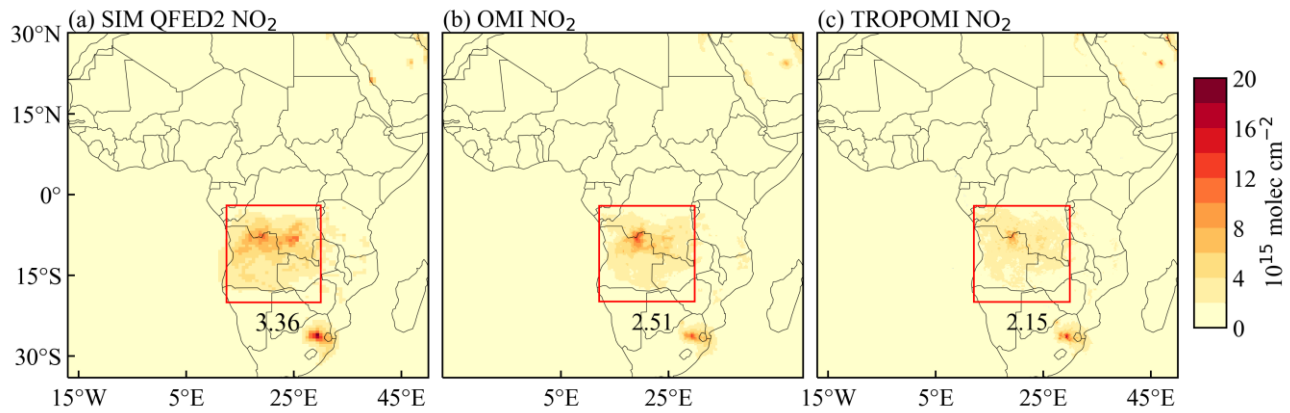
14 \*Correspondence to: keli@nuist.edu.cn



15

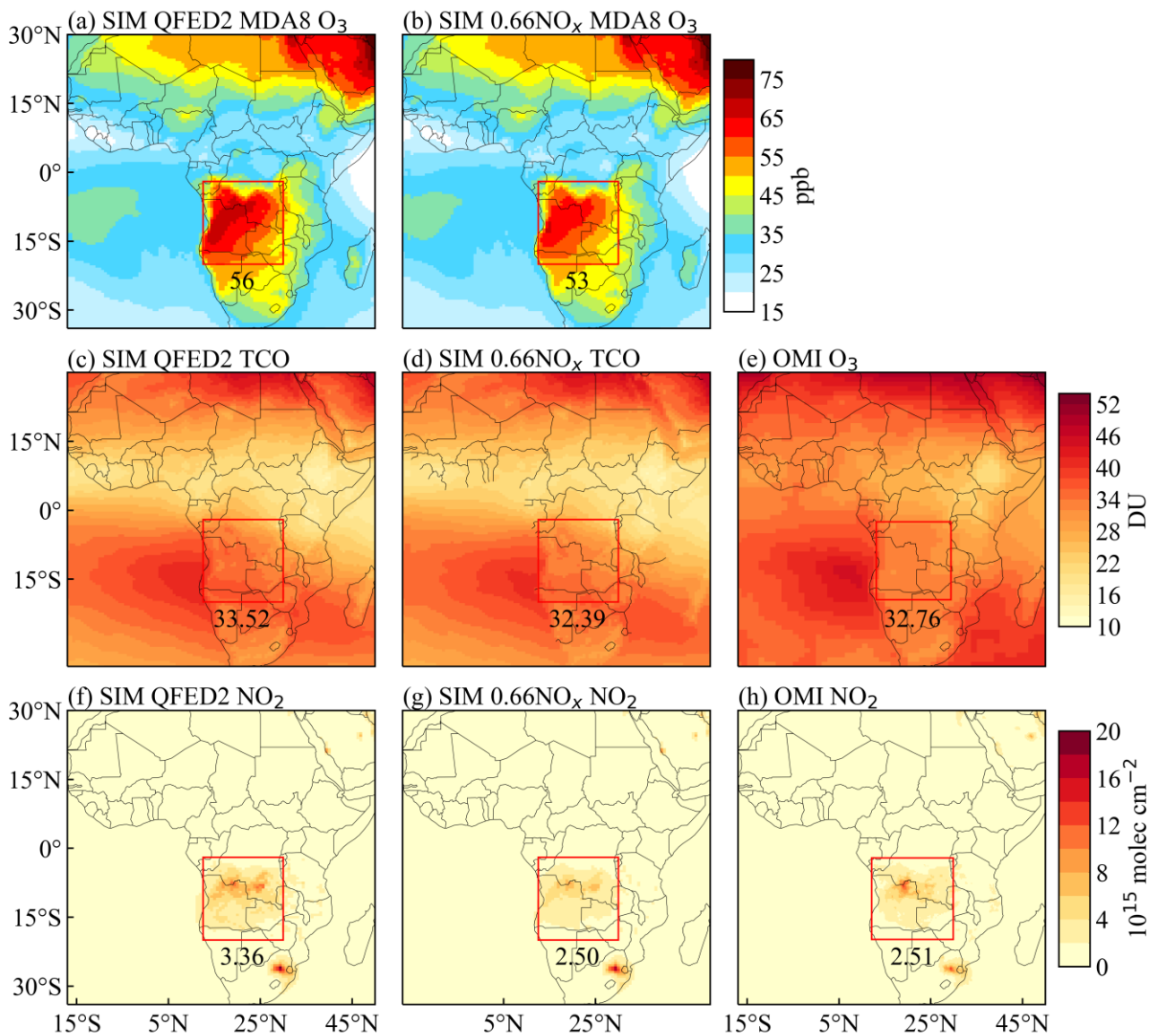
16 **Figure S1.** GEOS-Chem modelled surface ozone concentration obtained from the July 2019 benchmark experiment

17 (downloaded from [https://ftp.as.harvard.edu/gcgrid/geoschem/1mo\\_benchmarks/](https://ftp.as.harvard.edu/gcgrid/geoschem/1mo_benchmarks/)).

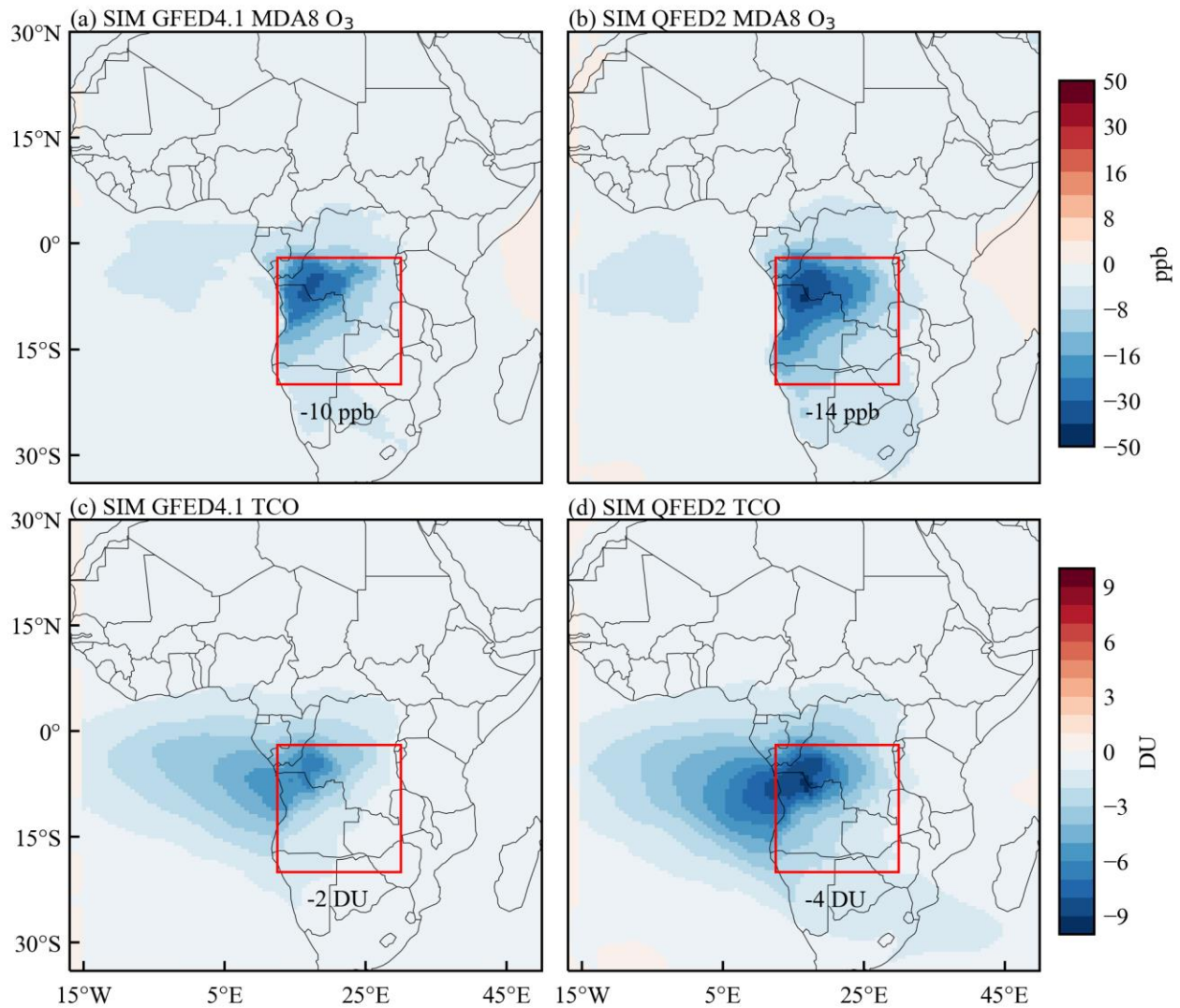


18

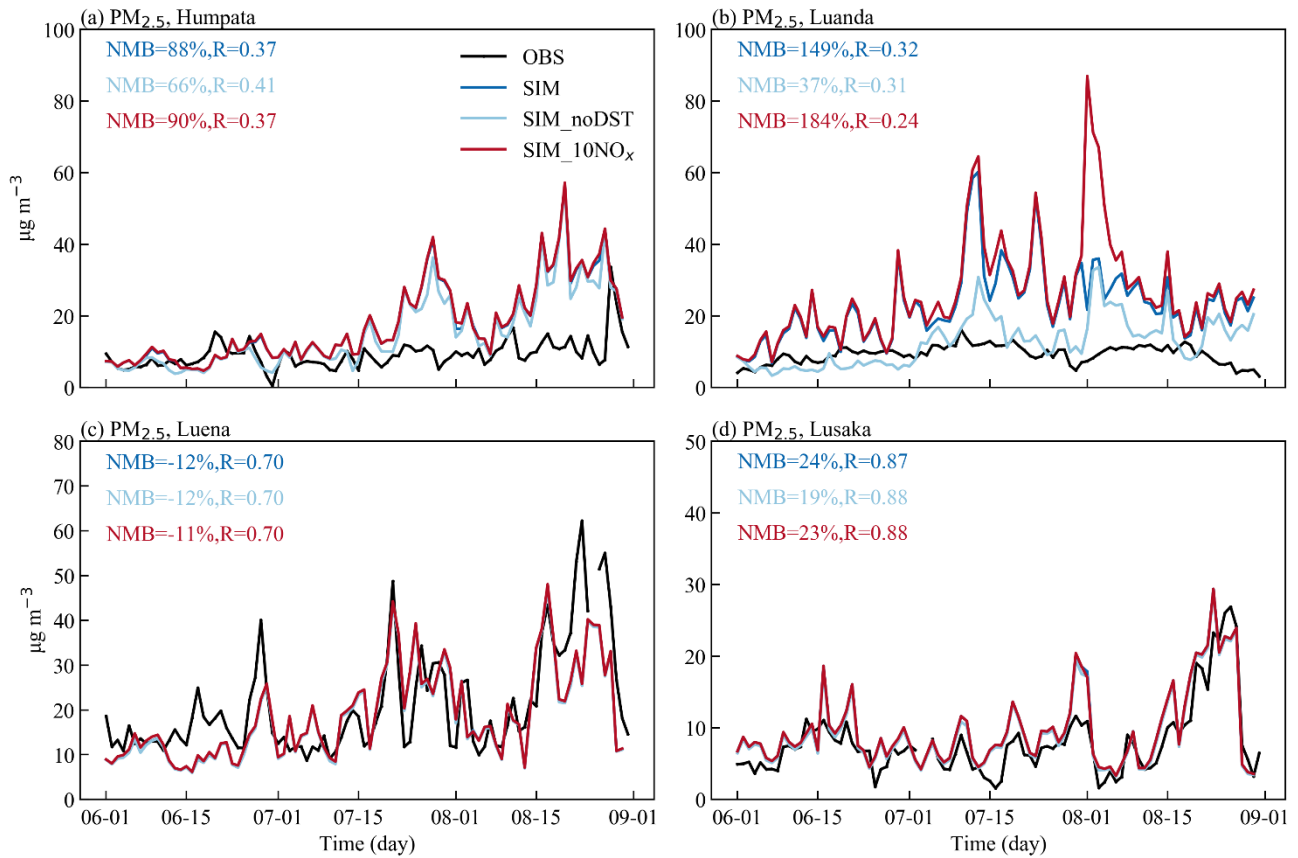
19 **Figure S2.** Comparison of the GEOS-Chem simulated NO<sub>2</sub> columns in Africa in July-August 2019 using the QFED2  
 20 inventory (a) with OMI (b) and TROPOMI (c). Numbers below the red boxes indicate the regional averages.



21  
 22 **Figure S3.** GEOS-Chem simulated surface ozone, tropospheric ozone columns, and NO<sub>2</sub> columns in Africa for July-August  
 23 2019 and its comparison with satellite data. The left panels are results from the baseline simulation; the middle panels are  
 24 results from the simulation with 34% reduction in NO<sub>x</sub> emissions from the QFED2 inventory; the right panels are results  
 25 from the satellite data.



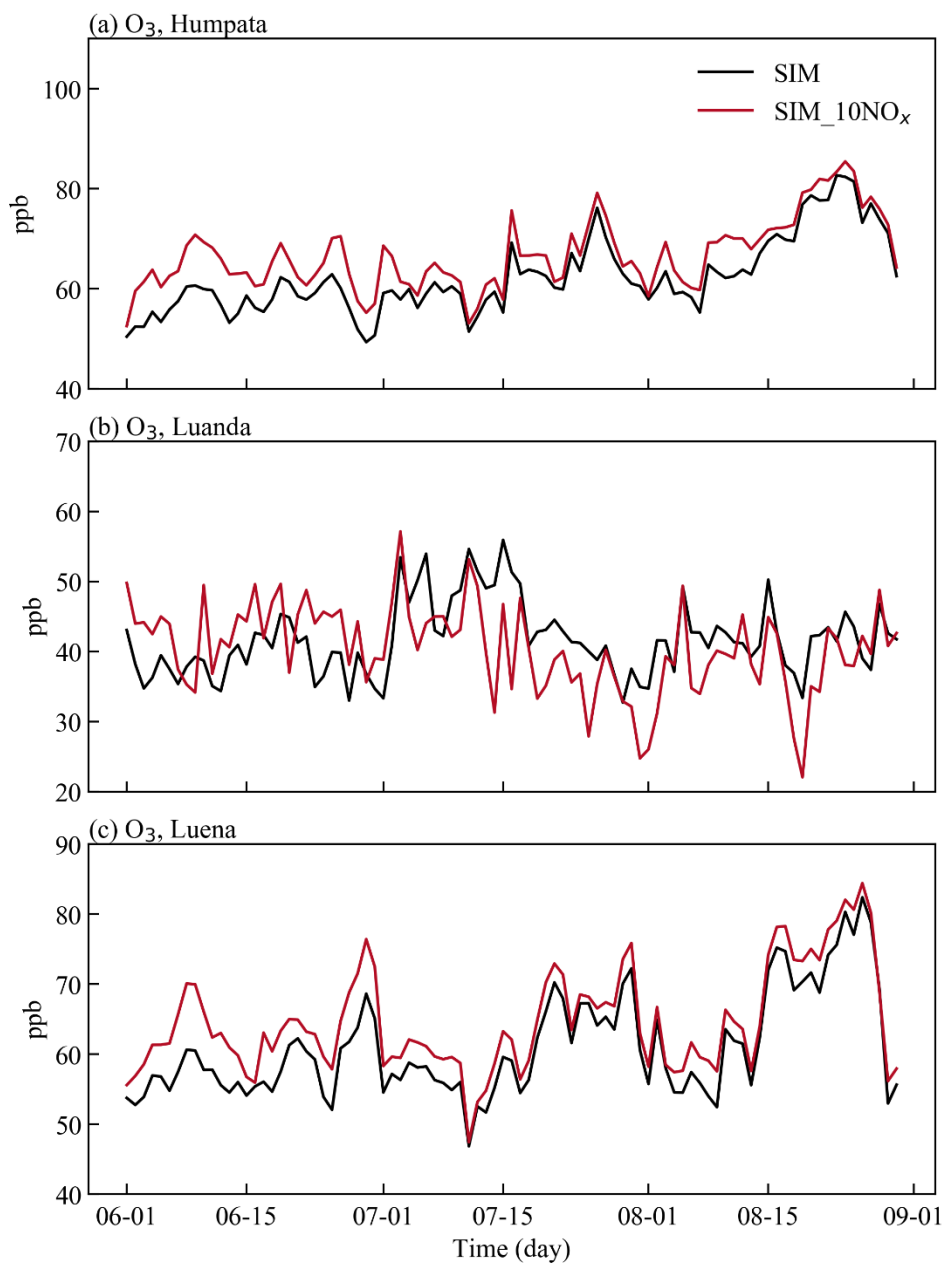
26  
 27 **Figure S4.** The simulated effects of aerosol chemistry on MDA8 ozone (top) and tropospheric ozone columns (bottom) in  
 28 July-August 2019 by using the GFED4.1 and QFED2, respectively.



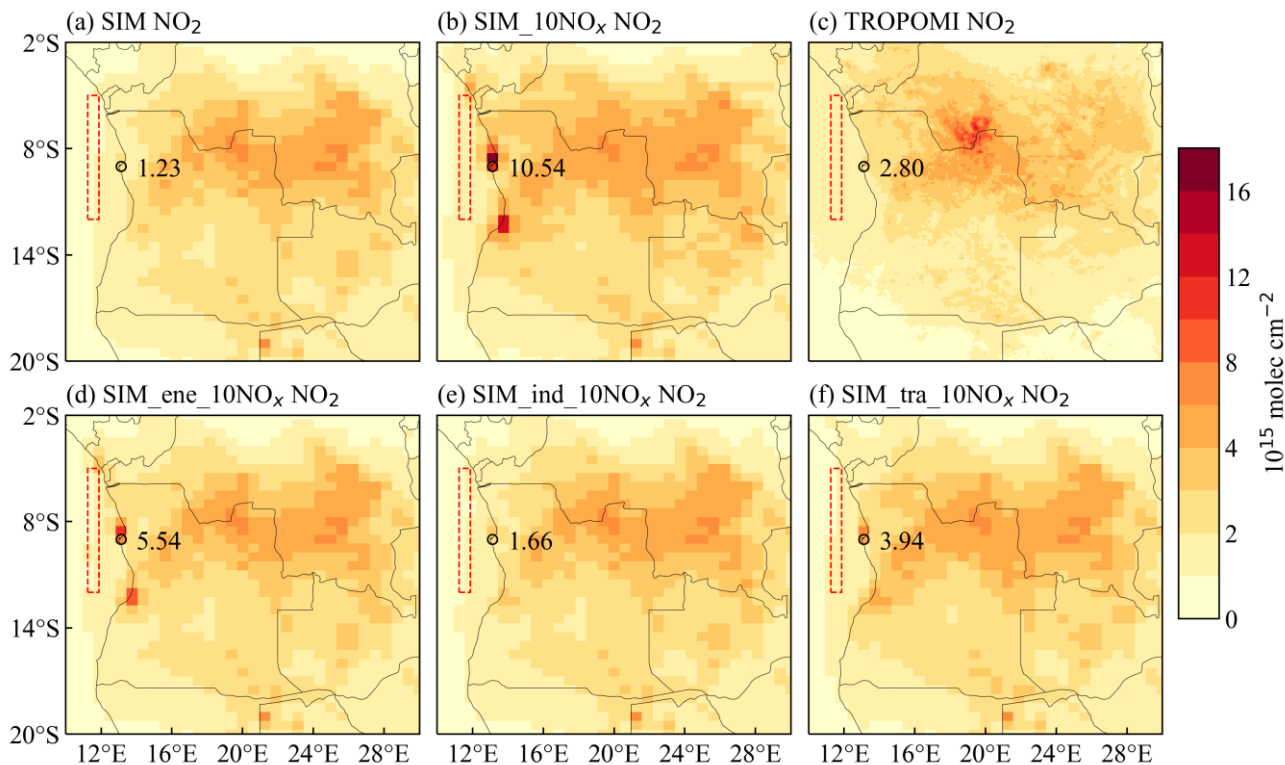
29

30

31 **Figure S5.** Time series of the simulated and observed (black) median daily  $PM_{2.5}$  concentrations for June-August 2023. a-  
 32 d are for Humpata, Luanda, Luena, and Lusaka, respectively. The plots labelled by the "SIM\_noDST" and "SIM\_10NO<sub>x</sub>"  
 33 are the  $PM_{2.5}$  concentration after removing dust aerosols and the  $PM_{2.5}$  concentrations when anthropogenic NO<sub>x</sub> emissions  
 34 were increased by a factor of 10 in CEDSV2.



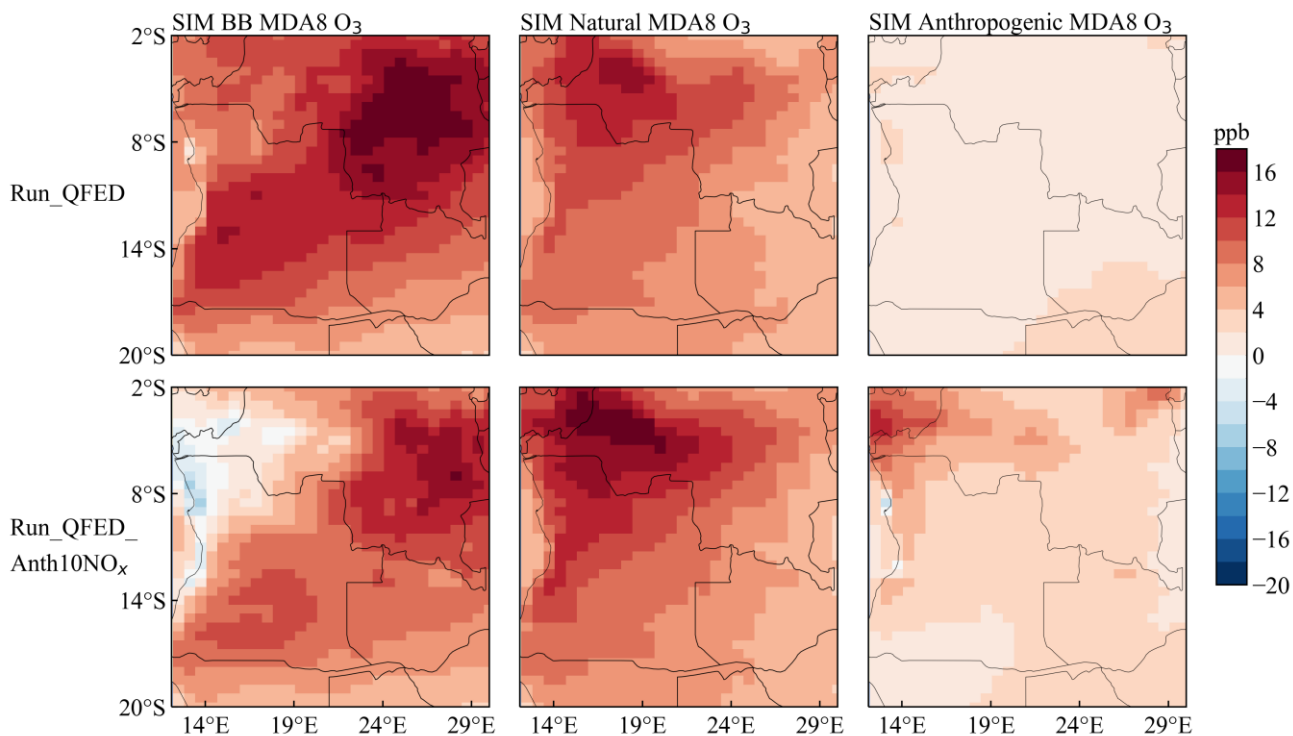
35  
 36 **Figure S6.** Time series of simulated June–August 2023 surface MDA8 ozone concentrations from the baseline simulation  
 37 (black) and the sensitivity simulation (red) in which anthropogenic NO<sub>x</sub> emissions were increased by a factor of 10 in  
 38 CEDSv2.



39

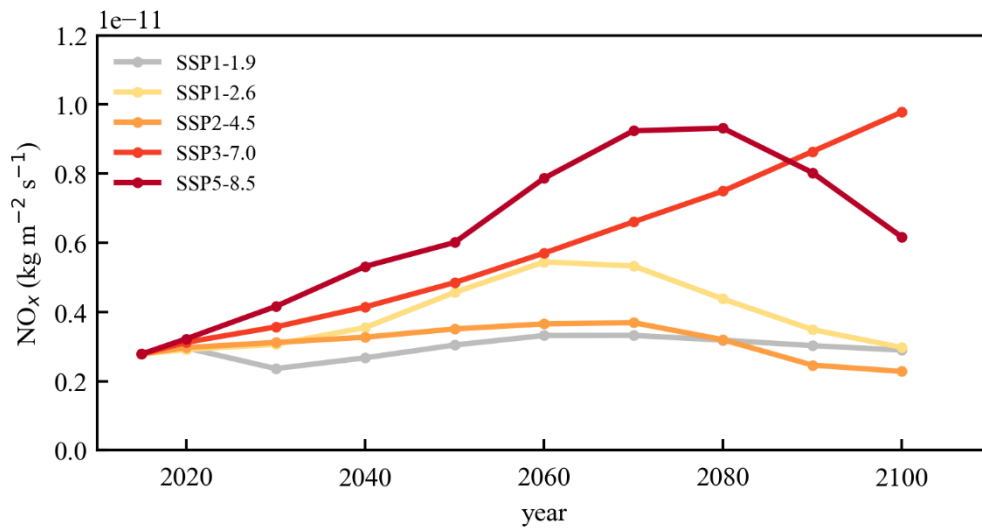
40 **Figure S7.** The observed and simulated tropospheric NO<sub>2</sub> columns in June-August 2023. (a) the baseline simulation with  
 41 QFED2 inventory. (b) the sensitivity simulation with anthropogenic NO<sub>x</sub> emissions increased by a factor of 10. (c)  
 42 TROPOMI data. (d-f) the sensitivity simulations with sectoral NO<sub>x</sub> emissions increased by a factor of 10 in energy, industry,  
 43 and transportation. The numbers in the plots are all the relative NO<sub>2</sub> columns enhancement in Luanda area. The dashed  
 44 boxes indicate the downwind background area, which is subtracted to obtain the relative NO<sub>2</sub> column concentration in  
 45 Luanda.





47

48 **Figure S8.** The simulated contributions to surface ozone in July-August 2019 from different sources, including biomass  
 49 burning emissions (left), natural emissions (middle), and anthropogenic emissions (right), under Run\_QFED simulation  
 50 (top) and under Run\_QFED\_Anth10NO<sub>x</sub> simulation (bottom) where anthropogenic NO<sub>x</sub> sources were increased by a factor  
 51 of 10. Here the natural emissions refer to the biogenic VOC and soil NO<sub>x</sub> emissions.



52  
53

**Figure S9.** Trends in NO<sub>x</sub> emission rates from anthropogenic sources under different future scenarios (Unit: kg m<sup>-2</sup> s<sup>-1</sup>).

54

**Table S1:** Satellite data used for this study

	Species	Spatial resolution	Time
OMI	O <sub>3</sub>	1° × 1.25°	July-August 2019
OMI	NO <sub>2</sub>	0.25° × 0.25°	2019-2020
OMI	HCHO	0.05° × 0.05°	July-August 2019
TROPOMI	NO <sub>2</sub>	0.125° × 0.125°	2018-2023
MODIS	AOD	1° × 1°	July-August 2019
MOPITT	CO	1° × 1°	July 2019

55